SEMARAK ILMU PUBLISHING

Journal of Advanced Research in Numerical Heat Transfer

Journal homepage:
https://semarakilmu.com.my/journals/index.php/arnht/index
ISSN: 2735-0142

Numerical Investigation on Thermal Performance of Various Designs Plate-Fin Heat Sinks Subject to Parallel and Impinging Flow

Muhammad Zarif Shaharudin[1], Syahar Shawal[1,*], Mazwan Mahat[1], Mohd Rosdzimin Abdul Rahman[2]

[1] School of Mechanical Engineering, College of Engineering, Universiti Teknologi MARA, 40450 Shah Alam, Selangor, Malaysia
[2] Department of Mechanical Engineering, Faculty of Engineering, Universiti Pertahanan Nasional Malaysia, Kem Sg. Besi, 57000, Kuala Lumpur, Malaysia

ARTICLE INFO

Article history:
Received 15 March 2023
Received in revised form 12 April 2023
Accepted 12 May 2023
Available online 30 June 2023

Keywords:
Plate-fin heat sinks; thermal performance; CFD

ABSTRACT

The electronic industry has been working for decades to improve the cooling efficiency of heat sinks by creating more advanced, efficient cooling technologies. However, heat dissipation remains the major problem in this highly competitive sector. Plate-fin heat sinks with and without fillet profiles were investigated and two new proposed designs for plate-fin heat sinks with half-round pins attached to the fin were developed in this study. Numerical analysis was performed using ANSYS FLUENT R21 to evaluate the thermal performance of the proposed designs. For the element optimization, the grid independency test analysis was performed to obtain the optimal number of elements. A constant heat flux of 18750 W/m2 was applied at the bottom plate of heat sinks as the input parameter and two different flow directions e.g., impinging flow and parallel flow at various mass flow rate was also applied to study the base temperature, thermal resistance and Nusselt number of these designs. The study has shown that plate-fin heat sinks with fillet profile and corrugated half-round pins (PFHS 4) subject to parallel flow and plate-fin heat sinks with fillet profile and symmetrical half-round pins (PFHS 3) subject to impinging flow exhibit better thermal performance over other configurations. Hence, these design configurations have a potential to be applied in the future.

1. Introduction

Due to recent advancements in semiconductor technology, power density in electronic and microelectronic equipment is increasing rapidly. The miniaturization of electronic devices has posed a difficulty for thermal management of such devices since overheating can lead to reduce in device performance. As a result, in a strong competitive electronic equipment business, increasing the heat transfer rate of such devices is crucial for long-term reliability. A heat sink is a component that allows more heat to be transferred away from a hot device. It achieves this by expanding the device's operating surface area and the amount of low-temperature fluid that flows through it [1]. Many

* *Corresponding author.*
E-mail address: syahar6595@uitm.edu.my (Syahar Shawal)

https://doi.org/10.37934/arnht.13.1.6680

industrial devices such as computer processors and air conditioning systems utilize heat sinks. Copper and aluminium are two typical metals used to manufacture heat sinks. To enhance the heat dissipation area, most heat sinks are built with fins that are attached to the heat sink base. Heat transfer improvement can be done in two ways: active and passive [2,3].

Natural convection cooling of electronic devices with finned heat sinks is a commonly practice in industry for various reasons including ease of manufacture, powerless operation, and high dependability. Heat sinks along with peripherals like jets and fans are always improving to fulfil the demand for more heat dissipation [4]. The parallel arrangement of rectangular cross section plate fins or pin fins on a flat base are two popular heat sink configurations. Plate-fin heat sinks are one type whereas pin-fin heat sinks are another.

Several studies show that comparisons of the efficiency of these configurations have been attempted. As example, F. Forghan *et al.,* [5] found that for low air velocities, the thermal performance of pin-fin heat sinks is significantly worse than plate-fin heat sinks. Contrary to popular belief, research has shown that the thermal performance of a pin-fin heat sink is better to that of a plate-fin heat sink under certain situations [6-8]. Kim *et al.,* [9] compared the thermal performance of plate-fin and pin-fin heat sinks subjected to impinging flow by performing experimental and analytical investigation. The pressure drop and thermal resistance of both configurations were predicted using a model based on the volume averaging approach. They discovered that when the heat sink's dimensionless length is high and the dimensionless pumping power is low, the optimized pin-fin heat sinks exhibit lower thermal resistance than the optimized plate heat sinks. Plate-fin heat sinks, on the other hand, have the least thermal resistance when the dimensionless pumping power is high and the dimensionless length of the heat sink is small.

A significant amount of research has also been focused on fully realizing the thermal performance enhancement that finned heat sinks offer by introducing new types of fin configurations which is not restricted to the typical types of heat sinks. For example, Hosseinirad *et al.,* [10] investigated the effect of two types of splitter shape namely wavy splitter and arched splitter on the cooling efficiency of thermal-hydraulic plate-fin heat sinks in both forward and backward arrangements were investigated. From the investigation, they found that arched splitter in a forwarding arrangement provide the lowest base temperature which resulting in a greater thermal performance. Other studies also included flared fins [5], oblique planar fins [11], rectangular perforation fins [12,13], square and circular perforation fins [14], square perforation fins [15-17], triangular perforations [18], radial heat sinks [19] and plate-fins with fillet profile [20].

Other than that, researchers have also been focused on the geometry of the heat sink's fin. For example, for popular plate-fin heat sinks, the effect of fin number and thickness of fin have been investigated analytically [21], the influence of the high and width of fin have been studied both numerically and experimentally [22], and the impact of fin number as well as both width and height of fin on the thermal performance of heat sinks have been explored experimentally [23] in previous works.

Furthermore, by establishing an effective flow direction can also improve the thermal performance of plate-fin heat sink. The effect of flow direction such as impinging flow and parallel flow on the enhancement of thermal performance and cooling efficiency of plate fin heat sinks has also been research by various researchers for instance in research paper in Ref. [24-30]. The former has been studied based on the Nusselt number [25], optimization of entropy generation [26] and a pressure drop model [27]. In case of plate-fin heat sinks by applying impinging flow, Biber [28] developed numerically obtained correlations for pressure loss coefficient and total heat transfer in a variable-length channel that covers a wide range of practical plate-fin heat sinks. Later on, Saini and Webb [29] validated Biber model [28] by experiments and made some modifications and

improvements. In another work, Duan and Muzychka [30] developed a simple semi-empirical model for predicting the pressure drop and the heat transfer coefficient of air-cooled plate-fin heat sinks.

To show the practicality of further enhancing the cooling effectiveness of plate-fin heat sinks with fillet profiles, more efficient designs must be developed. This paper intends to close this gap by evaluating the thermal performance of a new proposed design under both parallel and impinging flow conditions. As a result, this study provides a foundation for enhancing the thermal efficiency of plate-fin heat sinks with fillet profiles by proposing new basic designs that are easy to fabricate and implement than the novel designs previously stated. It would be possible to improve the cooling efficiency of plate-fin heat sinks in various flow directions using the proposed designs, which is important in many engineering applications. Therefore, this study aims to investigate the effect of fillet profile on heat transfer characteristics and evaluate the thermal performance of different design plate-fin heat sinks subjected to parallel and impinging flow.

2. Methodology

2.1 Geometrical Modelling

The model of the plate-fin heat sinks was created using CATIA V5 software. Later, the model will be transferred to the ANSYS FLUENT R21 for the simulation process. The parallel rectangular arrangement of fins on a flat base was used to model the plate-fin heat sinks. Figure 1(a) shows the dimensions of a plate-fin heat sink without a fillet profile. The base dimension is 40 mm x 39.7 mm in size, with a thickness of 5 mm. The channel width and fin thickness are assumed to remain constant over the length of the base and measure 3.3 mm and 1 mm respectively. An optimum fillet radius of 1.5 mm is used for the plate-fin heat sink with fillet profile shown in Figure 1 (b) as discussed in Ref. [20]. Besides that, the fin heights in Figure 1(a) and (b) varied by 25 mm and 28.6 mm respectively. This is due to the removed solid material from the fin base to create fillet was added to the fin height hence make the fin height for plate-fin heat sinks with fillet profile greater [20, 21]. In contrast to the previous study e.g. [20,21], the removed material from the fin base is attached to the plate-fins using half-round pins in the proposed designs as detailed in Ref. [31]. Table 1 provides the geometries dimension and arrangement in details.

Table 1
Geometry dimension and arrangement of different design of plate-fin heat sinks

Geometry Parameters	PFHS 1	PFHS 2	PFHS 3	PFHS 4
Length, L (mm)	39.7	39.7	39.7	39.7
Width, W (mm)	40.0	40.0	40.0	40.0
Height, H (mm)	25.0	28.6	25.0	25.0
Base Thickness, B (mm)	5.0	5.0	5.0	5.0
Number of Fins	10	10	10	10
Fin Thickness, F (mm)	1.0	1.27	1.27	1.27
Width Channel (mm)	3.3	3.0	3.0	3.0
Fillet Radius, R (mm)	-	1.5	1.5	1.5
Number of Half-Round Pin	-	-	108	108
Half-Round Pin Radius, HR (mm)	-	-	0.635	0.635

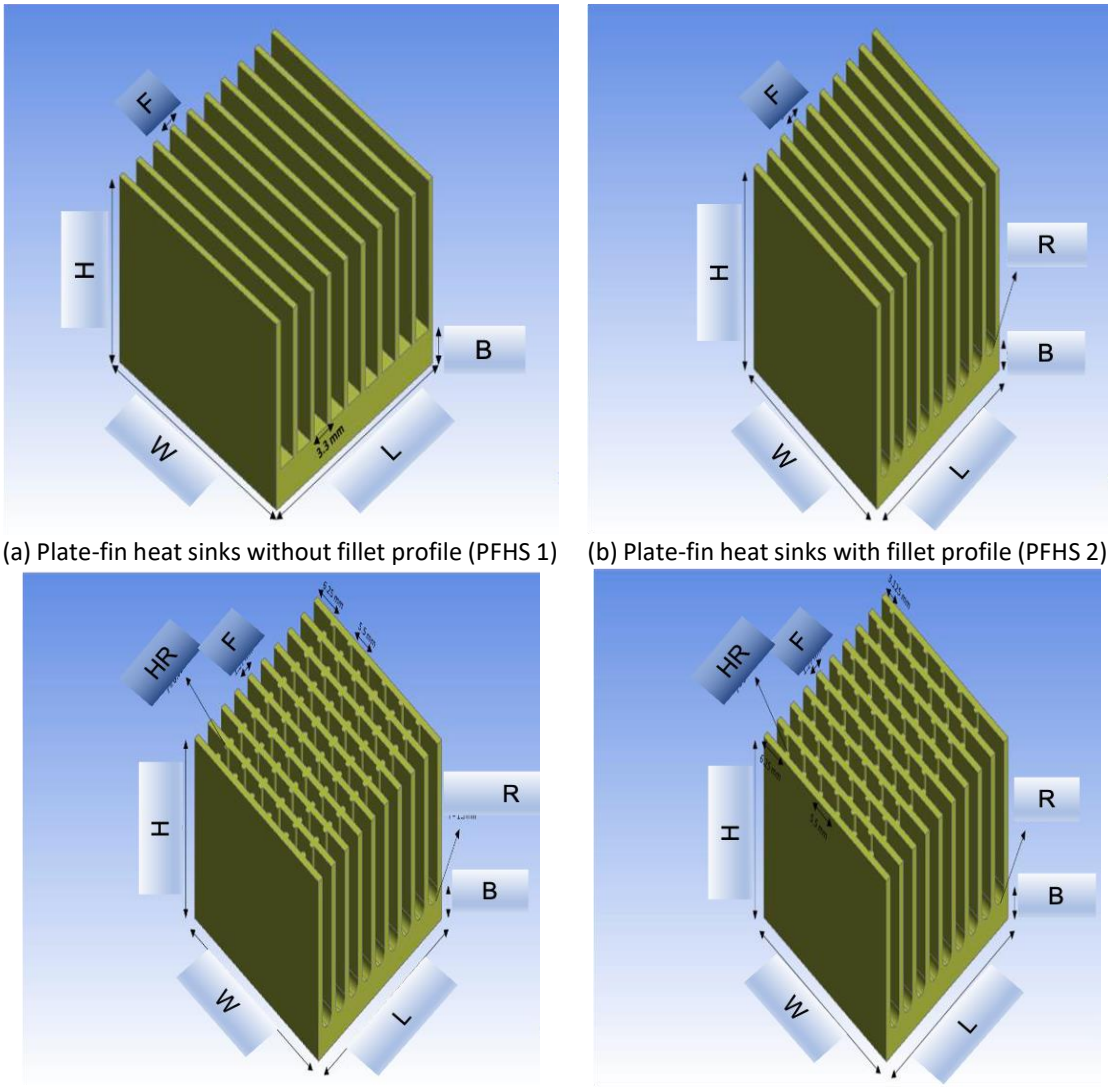

(a) Plate-fin heat sinks without fillet profile (PFHS 1)

(b) Plate-fin heat sinks with fillet profile (PFHS 2)

(c) Plate-fin heat sinks with fillet profile and symmetrical half-round pins (PFHS 3)

(d) Plate-fin heat sinks with fillet profile and corrugated half-round pins (PFHS 4)

Fig. 1. Geometrical model of plate-fin heat sinks

As shown in Figure 1 (a)-(d), four geometries including plate-fin heat sinks without fillet profile, plate-fin heat sinks with fillet profile, and new proposed designs of plate-fin heat sinks with fillet profile attached with symmetrical half-round pins in and corrugated half-round pins are investigated in this research. Both design with attached half-round pins are arranged in vertical arrangement. For the remainder of paper, the plate-fin heat sink subject to impinging flow is defined as air impinging on the heat sink along the y-axis direction and subsequently flowing parallel to the x-axis. Meanwhile, for the plate-fin heat sink subject to parallel flow, the air flows into the heat sink across the x-axis direction.

2.2 Grid Generation

ANSYS FLUENT R21 was used to create a computational grid and a three-dimensional discretized model of the plate-fin heat sinks in the pre-processor phase. The simulation results might be affected by the grids used. Since the thermal properties must be accurately evaluated, the complete geometry is discretized into finite volume hexahedral grids as in Ref. [21] (refer Figure 2).

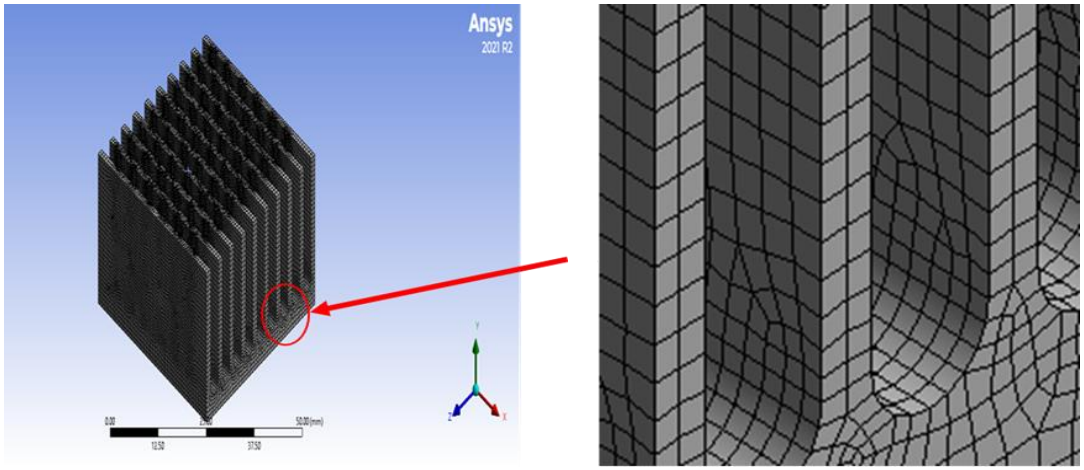

(a) General View (b) Zoom in View

Fig. 2. Meshing configuration

In addition, as the number of grid elements has a substantial influence on the numerical simulation outcome, mesh independency tests were done for different grid element numbers.

Table 2 shows the numerical results for the base temperature with different mesh configurations. It is clear that an increase in the number of grid elements does not result in a significant change in the base temperature. Since the differences between the results are still insignificant, a mesh with fewer grid components will be used for the remainder of the paper to speed up processing. The semi-implicit method for pressure linked equation (SIMPLE) algorithm is used for pressure-velocity coupling applications.

Table 2
Grid Independence Test

Plate-Fin Heat Sink	No of Element (10^6)	Base Temperature (K)	Temperature Difference
PFHS 1	0.79	390.24	-
	1.51	390.22	0.02
	2.82	389.94	0.28
PFHS 2	2.26	385.39	-
	5.77	385.52	0.13
	9.56	385.86	0.34
PFHS 3	2.08	369.25	-
	2.96	369.65	0.40
	3.64	369.76	0.11
PFHS 4	2.83	362.13	-
	3.10	362.85	0.72
	4.63	363.27	0.42

2.3 Boundary Conditions

In the solver execution phase of the development of CFD analysis, boundary conditions are considered similar to the experimental work published by Kim *et al.,* [9]. As in Ref. [9], the plate-fin heat sink was made of aluminum alloy 6061. A constant heat flux of 18750 W/m^2 was provided by electrical heater to warm up a plate-fin heat sink subject to impinging flow with variable values of inlet air flow i.e., (0.00092, 0.00218, 0.0033 and 0.00433) kg/s as shown in Figure 3.

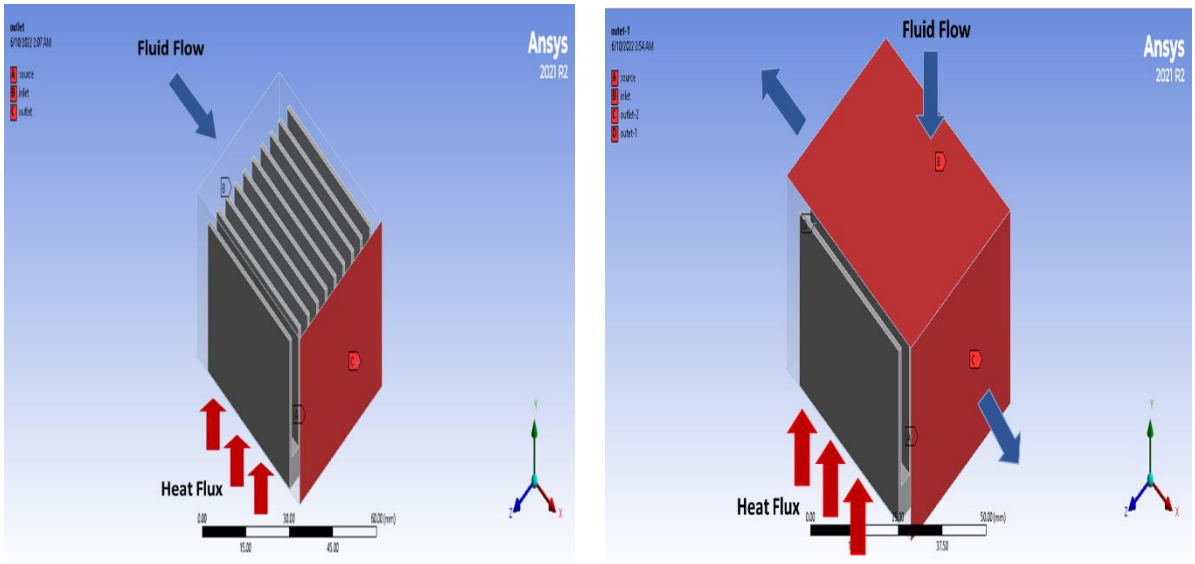

(a) Parallel flow (b) Impinging flow

Fig. 3. Numerical analysis of computational domain with boundary conditions

2.4 Governing Equations and Numerical Modeling

The governing equations for conservation of momentum, conservation of mass, and assuming the conjugate heat transfer i.e., Navier-Stokes, continuity, and energy equations are solved numerically to get the convective heat transfer characteristics. The bellow assumptions are considered:

I. The fluid flow is steady state, single phase and incompressible.
II. The flow is turbulent.
III. Three-dimension fluid-solid conjugate is considered.
IV. All physical properties of coolant air are depending on its mean temperature.

The Navier-Stokes equations across x, y and z directions are given as set of Eq. (1) [32]:

$$\begin{aligned}\nabla(\rho\vec{U}u) &= -\frac{\partial p}{\partial x}+\frac{\partial \tau_{xx}}{\partial x}+\frac{\partial \tau_{xy}}{\partial y}+\frac{\partial \tau_{zx}}{\partial z}\\ \nabla(\rho\vec{U}v) &= -\frac{\partial p}{\partial y}+\frac{\partial \tau_{xy}}{\partial x}+\frac{\partial \tau_{yy}}{\partial y}+\frac{\partial \tau_{zy}}{\partial z}\\ \nabla(\rho\vec{U}w) &= -\frac{\partial p}{\partial z}+\frac{\partial \tau_{xz}}{\partial x}+\frac{\partial \tau_{yz}}{\partial y}+\frac{\partial \tau_{zz}}{\partial z}\end{aligned} \quad (1)$$

where ρ is fluid density, $\vec{U}$ is the fluid velocity with the velocity components (u, v and w) in three directions, P is pressure and τ is the viscous stress tensor.
The energy equation is given by Eq. (2) as following [33]:

$$\nabla(\rho h\vec{U}) = -p\nabla\vec{U}+\nabla(k\nabla T)+\phi+s_h \quad (2)$$

where h is the enthalpy, k is thermal conductivity, T is temperature, ϕ is the dissipation term and s_h is the source term.

The energy equation for the conduction (solid), which occurs through the different materials is given by Eq. (3) as following [34]:

$$K_m = \left(\frac{\partial^2 T}{\partial x^2} + \frac{\partial^2 T}{\partial y^2} + \frac{\partial^2 T}{\partial z^2}\right) = 0 \tag{3}$$

where K_m is the thermal conductivity of the material.
Finally, the continuity equation is described by Eq. (4):

$$\nabla\left(\rho\vec{U}\right) = 0 \tag{4}$$

Based on the equations above, a separate solution is used. A sequential technique is utilized to solve the momentum and continuity equations. Due to the nonlinearity of the governing equations, the solution loop is iterated numerous times to obtain a convergent solution. The continuity, momentum, and energy equations are solved using the finite volume method, in which the integral version of the governing equations is solved using a continuum approach. The mathematical equations to describe temperature, pressure, and velocity are obtained in this manner. The convergence for momentum, mass and energy imbalance lesser than 10^6 is adopted.

2.5 Calculation Procedure

The average Nusselt number, $\overline{Nu}$, is based on the following Eq. (5):

$$\overline{Nu} = \frac{\bar{h}D_h}{K_a} \tag{5}$$

where $\bar{h}$ is the mean heat transfer coefficient, D_h is the hydraulic diameter of the inlet and K_a is the thermal conductivity of fluid (air). The latter is tabulated based on the mean temperature of air, T_m given by Eq. (6) as follows:

$$T_m = \frac{(T_{avr}+T_b)}{2} \tag{6}$$

where T_b the temperature of fin base while T_{avr} represent the average air temperature as defined in Eq. (7):

$$T_{avr} = \frac{(T_{out}+T_{in})_a}{2} \tag{7}$$

where T_{out} and T_{in} are outlet and inlet of air temperature respectively. In Eq. (5) the mean heat transfer coefficient, $\bar{h}$ is given by:

$$\bar{h} = \frac{Q}{A_T(T_b - T_m)} \tag{8}$$

where Q, A_T, T_b and T_m are the heat transfer rate to the air, the total area that is subjected to the air, the temperature of the fin base and the mean temperature of air respectively. In Eq. (8) the heat transfer rate to the air, Q and total cooling area, A_T can be expressed by Eq. (9) and Eq. (10) respectively:

$$Q = \dot{m}C_{Pa}(T_{out} + T_{in}) \tag{9}$$

where $\dot{m}$ is the mass flow rate and C_{Pa} is the specific heat of air.

$$A_T = WL + 2N_f H[L + t] + 2B[L + W] \tag{10}$$

where W and L are width and length of the heat sink respectively, N_f represents the number of fins, H, t and B are the height, thickness of fins and height of the base respectively.

The mean heat transfer coefficient, $\bar{h}$ can be calculated by substituting Eq. (9) and Eq. (10) into Eq. (8):

$$\bar{h} = \frac{\dot{m}C_{Pa}(T_{out}+T_{in})}{(WL+2N_f H[L+t]+2B[L+W])(T_b-T_m)} \tag{11}$$

Substituting Eq. (11) into Eq. (5) gives the average Nusselt number as prescribed by Eq. (12).

$$\overline{Nu} = \frac{\dot{m}C_{Pa}(T_{out}+T_{in})D_h}{(WL+2N_f H[L+t]+2B[L+W])(T_b-T_m)\,K_a} \tag{12}$$

The thermal resistance, R_{th} of plate-fin heat sinks in Eq. (13) is crucial for understanding the results of the CFD analysis reported in this paper.

$$R_{th} = \frac{1}{\bar{h}A_T} \tag{13}$$

3. Result & Discussion

3.1 Validation of the Study

Experimental work carried out by Kim *et al.,* [9] was compared with the numerical approach to validate its accuracy. The boundary conditions, geometry of plate-fin heat sink without fillet profile and direction of the air flow i.e., impinging flow is considered exactly similar to the experimental work carried out by Kim *et al.,* [9]. Thermal resistance at different mass flow rate were compared as presented in Figure 4.

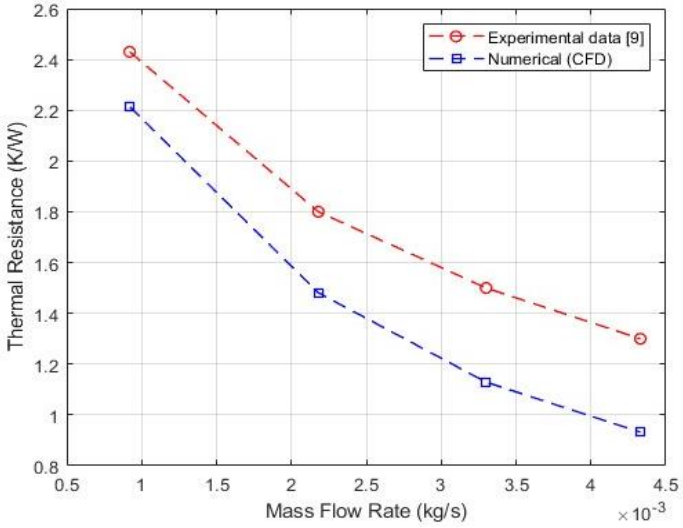

Fig. 4. Validation of numerical approach (CFD) at different mass flow rates for thermal resistance

As presented in Figure 4, the result of numerical approach (CFD) and the experimental work of Kim *et al.,* [9] shown slightly different. The explanation for the difference might be due to the measurement errors, and different numerical setup input parameters. However, it shown that the trend of the graph is much similar between these studies approach. It follows that the numerical approach that has been developed can be used for this study.

3.2 Comparison of Thermal Performance of Various Designs of Plate-fins Heat Sink

This section aims to compare the thermal performance of different proposed designs subject to both parallel and impinging flow. The comparison made is based on the base temperature, thermal resistance and Nusselt number of the plate-fin heat sink designs.

3.2.1 Parallel flow

The temperature contour of different plate-fin heat sink designs subjected to parallel flow at constant mass flow rate of 0.00092 kg/s are presented in Figure 5. As stated in Ref. [21], the larger in heat transfer area of plate-fin heat sinks with fillet profile (PFHS 2) resulted in the amount of heat removed from the hot region is higher compared to the plate-fin heat sinks without fillet profile (PFHS 1). Moreover, from the data obtained in the simulation analysis, the plate-fin heat sinks with fillet profile and corrugated half-round pins (PFHS 4) shown the best thermal performance as the heat distribution for this configuration has altered the most compared to other designs. Apart from this, even though the temperature contours do not show a significant change in different configurations but the maximum temperature measured is meaningfully different for the studied configurations i.e., 390 K, 382 K, 369 K and 362 K for Figure 5(a)-(d) respectively. Furthermore, the average temperature is lower for the inlet of air flow as illustrate in Figure 5. As the flow moving in x-direction, it is shown that the average temperature increases gradually. This is due to the effects of boundary layer thickness at the leading edge is thinner compared to at the trailing edge.

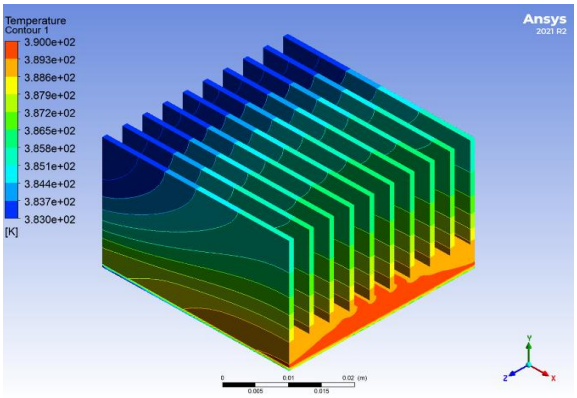

(a) Plate-fin heat sinks without fillet profile (PFHS 1)

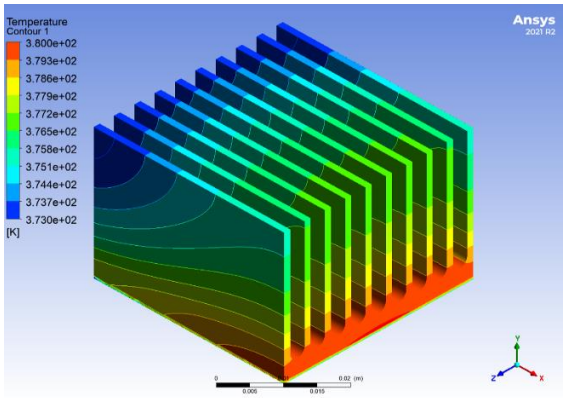

(b) Plate-fin heat sinks with fillet profile (PFHS 2)

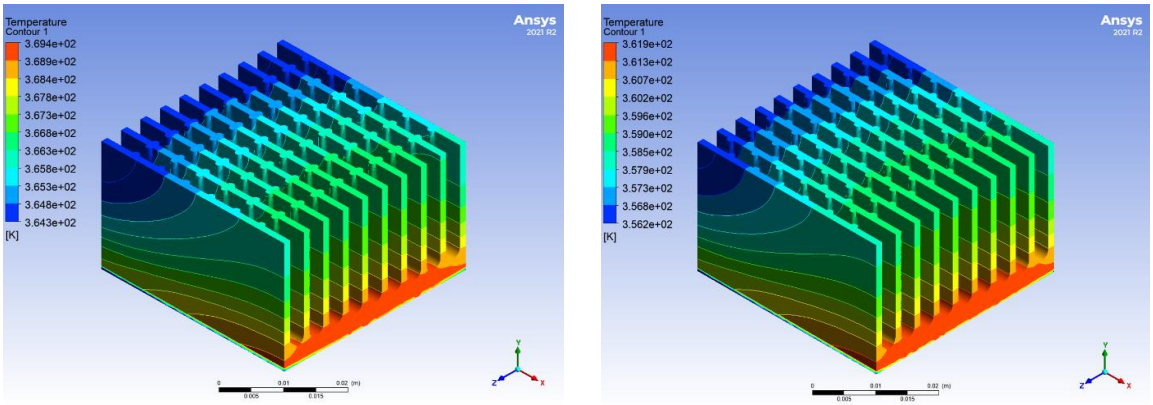

(c) Plate-fin heat sinks with fillet profile and symmetrical half-round pins (PFHS 3)

(d) Plate-fin heat sinks with fillet profile and corrugated half-round pins (PFHS 4)

Fig. 5. Temperature contour of the plate-fin heat sinks with different designs at a fix mass flow rate subjected to parallel flow

To investigate the thermal performance of plate-fin heat sinks with different attached half-round pins configuration subject to parallel flow, the changes in the base temperature, thermal resistance and Nusselt number of different designs are compared at various mass flow rates in Figure 6,7 and 8 respectively.

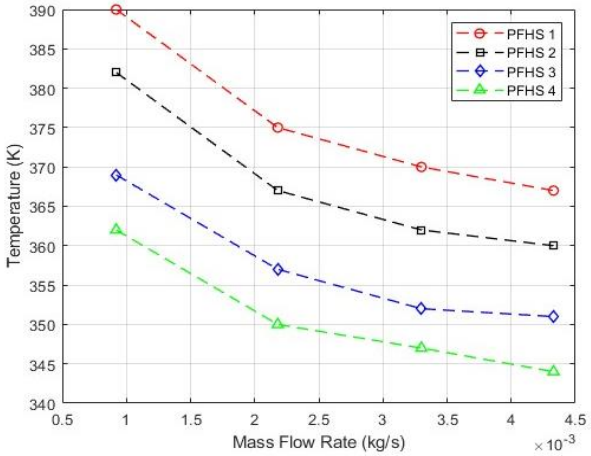

Fig. 6. The base temperature for different designs subjected to parallel flow at different flow rates

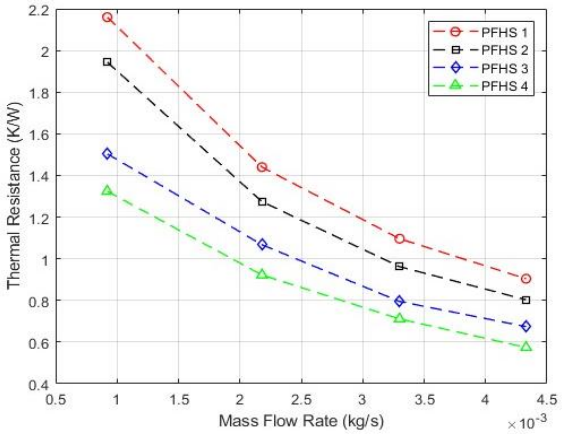

Fig. 7. The thermal resistance for different designs subjected to parallel flow at different flow rates

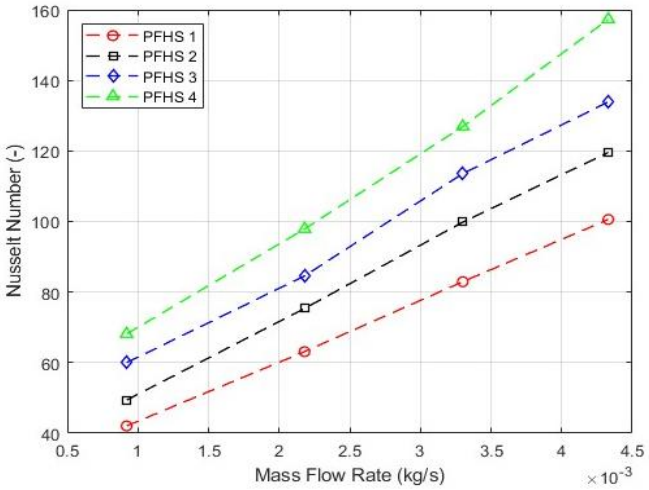

Fig. 8. Nusselt Number for different designs subjected to parallel flow at different flow rates

According to Figure 6 and 7, it shows that the higher the mass flow rates, the lower the base temperature and thermal resistance. Meanwhile, according to Figure 8, the Nusselt number increases as the mass flow rate increase which showing that the amount of heat is gradually dissipated from the hot region. The base temperature and thermal resistance with fillet profile and corrugated half-round pin (PFHS 4) are lower compared to plate-fin heat sinks with fillet profile (PFHS 2). On the other hand, the Nusselt number shows higher values. This represents that this design offer better thermal performance when subject to parallel flow.

3.2.2 Impinging flow

The temperature contour of different plate-fin heat sink designs subjected to impinging flow at constant mass flow rate of 0.00092 kg/s are presents in Figure 9.

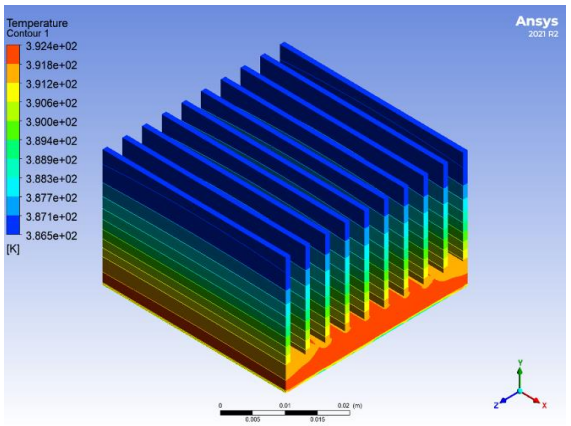

(a) Plate-fin heat sinks without fillet profile (PFHS 1)

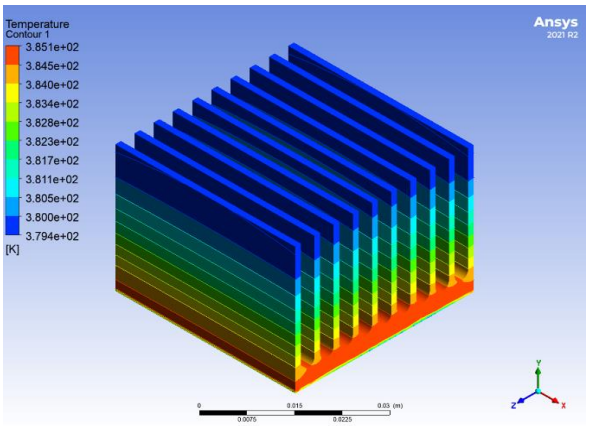

(b) Plate-fin heat sinks with fillet profile (PFHS 2)

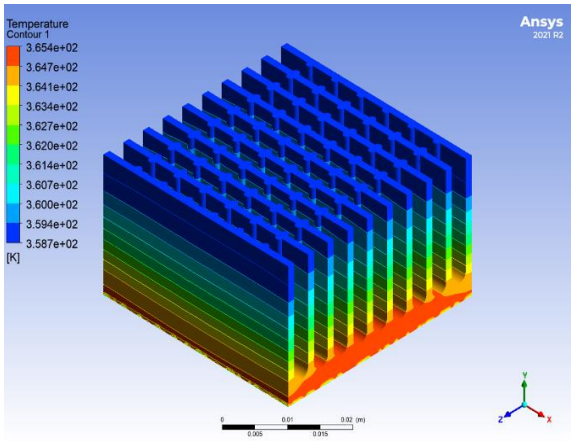

(c) Plate-fin heat sinks with fillet profile and symmetrical half-round pins (PFHS 3)

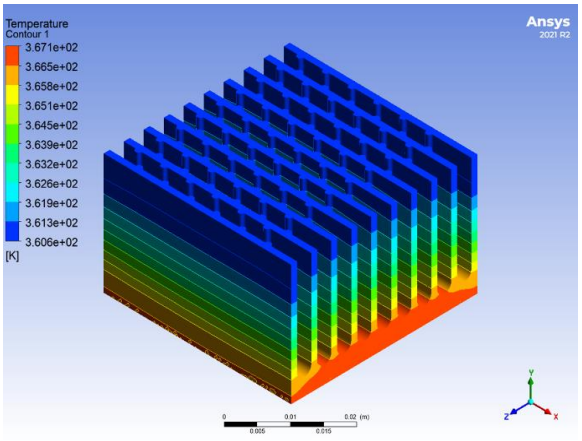

(d) Plate-fin heat sinks with fillet profile and corrugated half-round pins (PFHS 4)

Fig. 9. Temperature contour of the plate-fin heat sinks with different designs at a fixed mass flow subjected to impinging flow

From the data obtained in the simulation analysis, the plate-fin heat sinks with fillet profile and symmetrical half-round pins (PFHS 3) have the lowest base temperature compared to other designs. Apart from this, even though the temperature contours do not show a significant change in different configurations but the maximum temperature measured is meaningfully different for the studied configurations i.e., 392 K, 385 K, 365 K and 367 K for Figure 9(a)-(d) respectively. Furthermore, the average temperature is lower for the inlet of air flow which is at top region of the heat sink. As the flow moving downward in y-direction, the average temperature increase gradually and shows the highest value at the base of the heat sink. Besides, the temperature contours show less effective in heat distribution when compared to the results presented in Section 3.2.1.

As shown in Figure 10, plate-fin heat sinks with fillet profile and symmetrical half-round pins (PFHS 3) have the lowest base temperature among other designs when subjected to impinging flow at mass flow rate of 0.00092 kg/s. For the remainder of the result, it is expected that the temperature will decrease when the mass flow rate increase. It has been proven in the result presented in Section 3.2.1. Moreover, the thermal resistance is also expected to be the same pattern as in result presented in Section 3.2.1 where the thermal resistance will decrease as the mass flow rate is increased. Meanwhile, the Nusselt number will increase when the mass flow rate is increased.

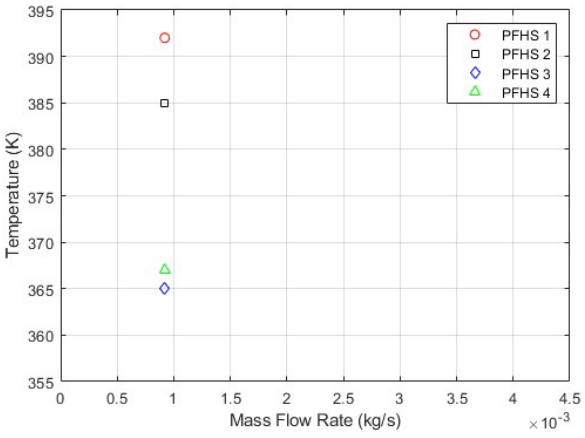

Fig. 10. Comparison of the base temperature for different designs subjected to impinging flow at a fixed mass flow rates of 0.00092 kg/s

4. Conclusions

Thermal performance of different design of plate-fin heat sinks with and without fillet profile subjected to parallel and impinging flow has been investigated and compared. The two new proposed designs for plate-fin heat sinks with fillet profile were introduced. The removed material from the fin base to create the fillet was re-used to form half-round pin that attached to the plate-fin, in symmetrical and corrugated arrangements. The results have shown that the plate-fin heat sink with fillet profile and corrugated half-round pins (PFHS 4) has the best thermal performance among other designs when subjected to parallel flow. The base temperature and thermal resistance are lower while the Nusselt number is higher when compared to plate-fin heat sinks with fillet profile (PFHS 2). Meanwhile, when they are subjected to impinging flow, the plate-fin heat sink with fillet profile and symmetrical half-round pin (PFHS 3) has the best thermal design among other designs. This study has provided a platform for further work, for example, investigating the heat transfer characteristics for both proposed designs experimentally which is useful for validation process of numerical work. Furthermore, studying the thermal performance with different pin shape i.e., square pin or hexagon with various pin parameters may also be included in further work.

Acknowledgement
This research was funded by a grant from Universiti Teknologi MARA, UiTM (MYRA Grant 600-RMC/GPM ST 5/3 (036/2021).

References

[1] Raunt, S. V., and B. S. Kothavale. "Study on thermal performance of micro fin heat sink under natural convection–A Review." *International Journal of Current Engineering and Technology* (2017): 257-261.
[2] Jadhav, Mahesh, Rahul Awari, Diksha Bibe, Amol Bramhane, and Mayura Mokashi. "Review on enhancement of heat transfer by active method." *International Journal of Current Engineering and Technology* 6 (2016): 221-225.
[3] Sonawane, Tejas, Prafulla Patil, Abhay Chavhan, and B. M. Dusane. "A review on heat transfer enhancement by passive methods." *International Research Journal of Engineering and Technology* 3, no. 9 (2016): 1567-1574.
[4] Bar-Cohen, Avram. "Thermal management of electronic components with dielectric liquids." *JSME International Journal Series B Fluids and Thermal Engineering* 36, no. 1 (1993): 1-25. https://doi.org/10.1299/jsmeb.36.1
[5] Forghan, Fariborz, Donald Goldthwaite, Matthew Ulinski, and Hameed Metghalchi. "Experimental and theoretical investigation of thermal performance of heat sinks." In *annual meeting for ISME, United States, May*. 2001.
[6] Kordyban, Tony, and Anthony J. Rafanelli. "Hot air rises and heat sinks: everything you know about cooling electronics is wrong." (1998): 395-395. https://doi.org/10.1115/1.2792653
[7] Kondo, Yoshihiro, and Hitoshi Matsushima. "Study of impingement cooling of heat sinks for LSI packages with longitudinal fins." *Heat Transfer-Japanese Research: Co-sponsored by the Society of Chemical Engineers of Japan and the Heat Transfer Division of ASME* 25, no. 8 (1996): 537-553. https://doi.org/10.1002/(SICI)1520-6556(1996)25:8<537::AID-HTJ4>3.0.CO;2-Y
[8] Li, Hung-Yi, Shung-Ming Chao, and Go-Long Tsai. "Thermal performance measurement of heat sinks with confined impinging jet by infrared thermography." *International Journal of Heat and Mass Transfer* 48, no. 25-26 (2005): 5386-5394. https://doi.org/10.1016/j.ijheatmasstransfer.2005.07.007
[9] Kim, Dong-Kwon, Sung Jin Kim, and Jin-Kwon Bae. "Comparison of thermal performances of plate-fin and pin-fin heat sinks subject to an impinging flow." *International Journal of Heat and Mass Transfer* 52, no. 15-16 (2009): 3510-3517. https://doi.org/10.1016/j.ijheatmasstransfer.2009.02.041
[10] Hosseinirad, E., M. Khoshvaght-Aliabadi, and F. Hormozi. "Effects of splitter shape on thermal-hydraulic characteristics of plate-pin-fin heat sink (PPFHS)." *International Journal of Heat and Mass Transfer* 143 (2019): 118586. https://doi.org/10.1016/j.ijheatmasstransfer.2019.118586
[11] Lin, Sheam-Chyun, Fu-Sheng Chuang, and Chien-An Chou. "Experimental study of the heat sink assembly with oblique straight fins." *Experimental Thermal and Fluid Science* 29, no. 5 (2005): 591-600. https://doi.org/10.1016/j.expthermflusci.2004.08.003

[12] Huang, Guei-Jang, Shwin-Chung Wong, and Chun-Pei Lin. "Enhancement of natural convection heat transfer from horizontal rectangular fin arrays with perforations in fin base." *International Journal of Thermal Sciences* 84 (2014): 164-174. https://doi.org/10.1016/j.ijthermalsci.2014.05.017
[13] AlEssa, Abdullah H., Ayman M. Maqableh, and Shatha Ammourah. "Enhancement of natural convection heat transfer from a fin by rectangular perforations with aspect ratio of two." *International Journal of physical sciences* 4, no. 10 (2009): 540-547.
[14] Dhanawade, Kavita H., Vivek K. Sunnapwar, and Hanamant S. Dhanawade. "Thermal analysis of square and circular perforated fin arrays by forced convection." *International Journal of Current Engineering and Technology* 2 (2014): 109-114.
[15] Huang, Ren-Tsung, Wen-Junn Sheu, and Chi-Chuan Wang. "Orientation effect on natural convective performance of square pin fin heat sinks." *International Journal of Heat and Mass Transfer* 51, no. 9-10 (2008): 2368-2376. https://doi.org/10.1016/j.ijheatmasstransfer.2007.08.014
[16] AlEssa, Abdullah HM. "Augmentation of fin natural convection heat dissipation by square perforations." *Journal of mechanical engineering and automation* 2, no. 2 (2012): 1-5. https://doi.org/10.5923/j.jmea.20120202.01
[17] Liu, Minghou, Dong Liu, Sheng Xu, and Yiliang Chen. "Experimental study on liquid flow and heat transfer in micro square pin fin heat sink." *International Journal of Heat and Mass Transfer* 54, no. 25-26 (2011): 5602-5611. https://doi.org/10.1016/j.ijheatmasstransfer.2011.07.013
[18] AlEssa, Abdullah H., and Mohamad I. Al-Widyan. "Enhancement of natural convection heat transfer from a fin by triangular perforation of bases parallel and toward its tip." *Applied mathematics and mechanics* 29 (2008): 1033-1044. https://doi.org/10.1007/s10483-008-0807-x
[19] Freegah, Basim, Ammar A. Hussain, Abeer H. Falih, and Hossein Towsyfyan. "CFD analysis of heat transfer enhancement in plate-fin heat sinks with fillet profile: Investigation of new designs." *Thermal Science and Engineering Progress* 17 (2020): 100458. https://doi.org/10.1016/j.tsep.2019.100458
[20] Wong, Kok-Cheong, and Sanjiv Indran. "Impingement heat transfer of a plate fin heat sink with fillet profile." *International Journal of Heat and Mass Transfer* 65 (2013): 1-9. https://doi.org/10.1016/j.ijheatmasstransfer.2013.05.059
[21] Hussain, Ammar A., Basim Freegah, Basima Salman Khalaf, and Hossein Towsyfyan. "Numerical investigation of heat transfer enhancement in plate-fin heat sinks: Effect of flow direction and fillet profile." *Case Studies in Thermal Engineering* 13 (2019): 100388. https://doi.org/10.1016/j.csite.2018.100388
[22] Elnaggar, Mohamed HA. "Heat transfer enhancement by heat sink fin arrangement in electronic cooling." *Heat Transfer* 2, no. 3 (2015).
[23] Li, Hung-Yi, Kuan-Ying Chen, and Ming-Hung Chiang. "Thermal-fluid characteristics of plate-fin heat sinks cooled by impingement jet." *Energy Conversion and Management* 50, no. 11 (2009): 2738-2746. https://doi.org/10.1016/j.enconman.2009.06.030
[24] Li, Hung-Yi, Ming-Hung Chiang, Chih-I. Lee, and Wen-Jei Yang. "Thermal performance of plate-fin vapor chamber heat sinks." *International Communications in Heat and Mass Transfer* 37, no. 7 (2010): 731-738. https://doi.org/10.1016/j.icheatmasstransfer.2010.05.015
[25] Teertstra, P., M. M. Yovanovich, and J. R. Culham. "Analytical forced convection modeling of plate fin heat sinks." *Journal of Electronics Manufacturing* 10, no. 04 (2000): 253-261. https://doi.org/10.1142/S0960313100000320
[26] Khan, Waqar A., J. Richard Culham, and M. Michael Yovanovich. "Optimization of pin-fin heat sinks using entropy generation minimization." *IEEE Transactions on Components and Packaging Technologies* 28, no. 2 (2005): 247-254. https://doi.org/10.1109/TCAPT.2005.848507
[27] Copeland, David. "Optimization of parallel plate heatsinks for forced convection." In *Sixteenth Annual IEEE Semiconductor Thermal Measurement and Management Symposium (Cat. No. 00CH37068)*, pp. 266-272. IEEE, 2000.
[28] Biber, Catharina R. "Pressure drop and heat transfer in an isothermal channel with impinging flow." *IEEE Transactions on Components, Packaging, and Manufacturing Technology: Part A* 20, no. 4 (1997): 458-462. https://doi.org/10.1109/95.650935
[29] Saini, Manish, and Ralph L. Webb. "Validation of models for air cooled plane fin heat sinks used in computer cooling." In *ITherm 2002. Eighth Intersociety Conference on Thermal and Thermomechanical Phenomena in Electronic Systems (Cat. No. 02CH37258)*, pp. 243-250. IEEE, 2002.
[30] Duan, Zhipeng, and Y. S. Muzychka. "Pressure drop of impingement air cooled plate fin heat sinks." (2007): 190-194. https://doi.org/10.1115/1.2721094
[31] Freegah, Basim, Ammar A. Hussain, Abeer H. Falih, and Hossein Towsyfyan. "CFD analysis of heat transfer enhancement in plate-fin heat sinks with fillet profile: Investigation of new designs." *Thermal Science and Engineering Progress* 17 (2020): 100458. https://doi.org/10.1016/j.tsep.2019.100458

[32] Hochstein, John I., and Andrew L. Gerhart. *Young, Munson and Okiishi's A Brief Introduction to Fluid Mechanics*. John Wiley & Sons, 2021.
[33] Hoffmann, Klaus A., and Steve T. Chiang. "Computational fluid dynamics volume I." *Engineering education system* (2000).
[34] Blazek, Jiri. *Computational fluid dynamics: principles and applications*. Butterworth-Heinemann, 2015. https://doi.org/10.1016/B978-0-08-099995-1.00012-9